

Physics-Based Modeling of Selective Catalytic Reduction System and Corresponding Reduced Order Dynamics

Ram Chander Bhaskara^{1*}, Sabareish P¹, Srinivas M¹ and Umapathy M²

¹National Institute of Technology, Tiruchirappalli, India

²Instrumentation and Control Engineering, National Institute of Technology, Tiruchirappalli, India

Abstract

This paper focuses on developing the physics-based model of the SCR system. Through the use of first principles, governing equations of the SCR physics-based model are achieved. The SCR system is modeled in a series of segments. The main reactions are ammonia adsorption, desorption, reduction, and ammonia oxidation. The resulting non-linear partial differential equations are discretized and linearized to obtain a state space model. The model is extended to a sufficiently large order to achieve accuracy. The developed model is analyzed and the system dynamics are studied, validated using simulation studies of a Urea-SCR system. In addition, reduced order dynamics of the SCR system are also analyzed in this paper.

Keywords: Emission reduction in diesel engines; After-treatment system; SCR; Modelling; Physics based SCR model

Introduction

Selective Catalytic Reduction (SCR) system is used to reduce the oxides of nitrogen NO and NO₂ to N₂ and water (H₂O). The use of SCR system to reduce NO_x emissions has been in place since Engelhard Corporation, in 1957, patented this method in the United States.

SCR technology was implemented on a commercial vehicle to meet the EURO IV regulation. Since then the use of SCR in automotive applications has been increasing. There are other technologies such as EGR (Exhaust Gas Recirculation) and LNT (Lean NO_x trap) which are used to reduce the NO_x emissions.

The SCR system is popular because the engine can be tuned to operate at a very high efficiency which implies higher flame temperatures without compromising the NO_x conversion. There are combinations of EGR+SCR, pure SCR, and pure EGR which have been used in the past. For EURO VI and above emission regulations SCR+EGR and SCR only solution are viable options to reduce NO_x without compromising on the engine efficiency. FPT was the first to introduce an SCR only solution. Since then a number of other manufacturers like Scania have opted for the SCR only option [1-8].

Selective Catalytic Reduction

SCR stands for selective catalytic reduction. SCR catalysts remove nitrogen oxides (NO_x) using a reducing agent ammonia (NH₃). An SCR catalyst is used to speed up the reactions and to provide a surface on which the reactions take place. As mentioned earlier the reducing agent is carried on board the vehicle as an aqueous solution containing 32.5% urea. This solution is called AdBlue and is used as the storage and transportation is easier.

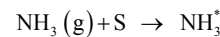
SCR Kinetic Model

The NH₃ storage model consists of modeled reaction rates. These reaction rates are used to calculate the gas phase concentrations of NO_x as well as NH₃. Detailed kinetic models such as the ones used by catalyst manufacturers such as Johnson Matthey and BASF are very detailed. They usually include the reaction rates of all the reactions that occur or certain side reactions that might occur inside an SCR converter.

The chemical kinetics in an SCR system involves the following reactions:

Adsorption and desorption of NH₃ onto the surface of the catalytic converter

This mechanism can be depicted by the following reaction:

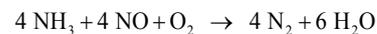


Where S in equation denotes a free site on the surface of the catalytic converter and NH₃^{*} denotes an ammonia molecule adsorbed onto the surface of the catalytic converter. A free site on a catalytic surface is an empty void. This is formed due to the adsorbent (the coating of the catalytic converter in this case) not being completely surrounded by the other adsorbent atoms. This empty site is occupied by the ammonia molecules. The forward reaction in the equation denotes adsorption of the ammonia molecule while the reverse denotes desorption of NH₃^{*} molecule.

SCR reactions

There are mainly three important chemical reactions that occur between the ammonia stored in the catalyst and the NO_x entering the catalyst.

The first SCR reaction is called the standard SCR. This reaction is depicted below:



In this reaction, gas phase NO_x, Oxygen, and adsorbed Ammonia react with each other to produce water and Nitrogen. This reaction occurs dynamically, and the goal of this thesis is to determine a model that captures this conversion accurately, thereby setting the stage for a

***Corresponding author:** Ram Chander Bhaskara, National Institute of Technology Tiruchirappalli, India, Tel: +91-8754306611, E-mail: ramchanderbhaskara@gmail.com, umapathy@nitt.edu

Received: October 18, 2018; **Accepted:** October 26, 2018; **Published:** November 02, 2018

Citation: Bhaskara RC, Sabareish P, Srinivas M, Umapathy M (2018) Physics-Based Modeling of Selective Catalytic Reduction System and Corresponding Reduced Order Dynamics. Int J Adv Technol 9: 213. doi:10.4172/0976-4860.1000213

Copyright: © 2018 Bhaskara RC, et al. This is an open-access article distributed under the terms of the Creative Commons Attribution License, which permits unrestricted use, distribution, and reproduction in any medium, provided the original author and source are credited.

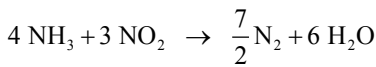
control design that allows the determination of an optimal profile of the Ammonia input that allows a maximum NO_x conversion.

Another important SCR reaction is called the *Fast SCR*. This reaction is depicted below:



The above equation consumes one mole of NH₃ per mole of NO_x and is faster compared to the standard SCR. The Diesel Oxidation Catalyst (DOC) alters the ratio of NO/NO₂. The ratio of NO/NO₂ in the engine out NO_x will thus change after the DOC. This will ensure that a major portion of the NO_x gets converted through the fast SCR reaction. The fast SCR is usually the dominant reaction when the ratio of NO/NO₂ is close to one.

The last SCR reaction is called the *Slow SCR* and is shown below:



The slow SCR reaction is usually not relevant as it can be neglected. The reaction rate of the slow SCR becomes significant when the entire NO is consumed inside the catalytic converter.

SCR temperature model

The SCR model also consists of a sub-model that calculates the temperature dynamics of the SCR system. The temperature model is based on simple heat balance. The SCR is assumed to be a perfect heat exchanger. This implies that the temperature exhaust gas leaving the SCR is equal to the temperature of the SCR. The SCR is assumed to be very well insulated therefore convective and radiative losses are ignored.

Modeling the SCR System

A physical and chemical phenomenon in the catalyst

When exhaust gas containing NH₃ and NO_x is supplied into the channel, several physical and chemical phenomena occur. The first phenomenon is a diffusion of species of NH₃ and NO_x between flowing gas and stationary gas in the wash coat which is then followed by chemical reactions between molecules on the surface of the catalyst. The third phenomenon is heat transfer between the flowing gas and the wash coat/structure. To model these phenomena, we need at two energy equations for the gas and the wash coat/structure and species equations for each species in the flowing channel, the stationary gas of the wash coat, and on the catalyst. Below are the energy equations to calculate wall temperature and gas temperature (Figure 1).

$$\rho_w A_w C_{p,w} \frac{\partial T_w}{\partial t} = -h \cdot P (T_w - T_g) + s \sum_j R_j \Delta H_j$$

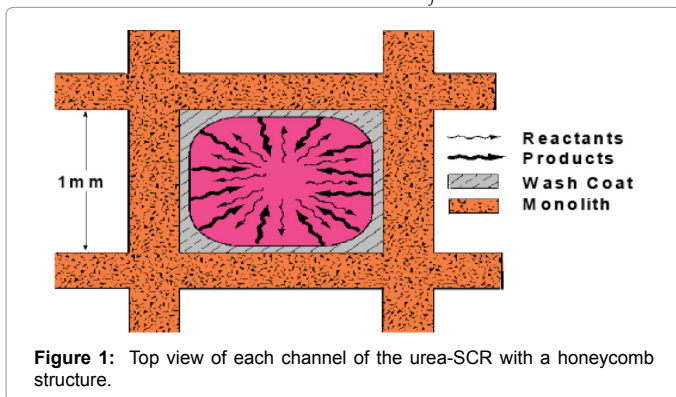


Figure 1: Top view of each channel of the urea-SCR with a honeycomb structure.

$$\rho_g A_g C_{p,g} \frac{\partial T_g}{\partial t} + \rho_g A_g C_{p,g} u \frac{\partial T_g}{\partial x} = -h \cdot P (T_g - T_w)$$

The below equations represent equations of *i*th species in the flowing gas and the stationary gas in a wash coat, and on the catalyst surface, respectively.

$$A_g \frac{\partial C_i}{\partial t} + A_g u \frac{\partial C_i}{\partial x} = -D \cdot P (C_i - C_{i(wt)})$$

$$A_{wt} \frac{\partial C_{i(wt)}}{\partial t} = D \cdot P (C_i - C_{i(wt)}) - s \sum_j R_{j-i}$$

$$A_w \frac{\partial C_{i(s)}}{\partial t} = s \sum_j R_{j-i}$$

Governing Equations

Below are the energy equations of wall and gas, respectively.

$$\frac{\partial T_g}{\partial x} = -\frac{h \cdot P}{\rho_g A_g C_{p,g} u} (T_g - T_w) \tag{1}$$

$$\frac{\partial T_w}{\partial x} = -\frac{h \cdot P}{\rho_w A_w C_{p,w}} (T_w - T_g) \tag{2}$$

Below are the NH₃ and NO species equations of flowing gas in a channel.

$$\frac{\partial C_{NH_3}}{\partial x} = \frac{s}{A_g u} (-R_a + R_d) = \frac{s}{A_g u} \left(-P_a (1 - \theta) C_{NH_3} + P_d \exp\left(-\frac{E_{d0}(1 - \alpha\theta)}{R \cdot T_w}\right) \theta \right) \tag{3}$$

$$\frac{\partial C_{NO}}{\partial x} = \frac{s}{A_g u} (-R_r) = \frac{s}{A_g u} \left(-P_r \exp\left(-\frac{E_r}{R \cdot T_w}\right) \cdot \theta \cdot C_{NO} \right) \tag{4}$$

The species equation of adsorbed Ammonia on the surface of the catalyst. θ is the fraction loading of Ammonia onto the catalyst and defined by $\frac{C_{NH_3}}{\Omega}$ in which Ω is the number of reaction-sites per volume of wash coat (Figure 2).

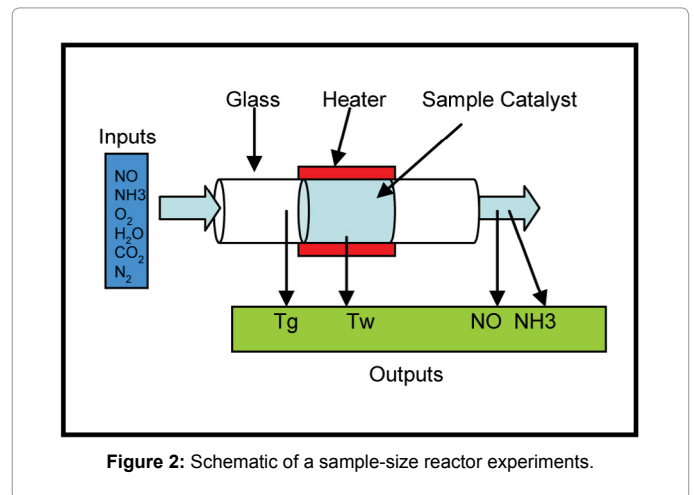


Figure 2: Schematic of a sample-size reactor experiments.

$$\frac{\partial \theta_i}{\partial t} = (R_{a,i} - R_{d,i} - R_{r,i} - R_{o,i})$$

$$= \begin{pmatrix} p_a(1-\theta)C_{NH_3,i} - p_d \exp\left(-\frac{E_{d0}(1-\alpha\theta_i)}{R \cdot T_{w,i}}\right) \theta_i \\ -p_r \exp\left(-\frac{E_r}{R \cdot T_{w,i}}\right) \cdot \theta_i \cdot C_{NO,i} - p_o \exp\left(-\frac{E_o}{R \cdot T_{w,i}}\right) \cdot \theta_i \cdot C_{O_2} \end{pmatrix} \quad (5)$$

Linearized Model

To derive state space form for the whole system, we first discretized equations in the spatial domain, and derived state space form equation for governing equations which are continuous in time for each segment. Then, every state equation for each segment is assembled into one large state space equation (Figure 3).

Discretization in space

To derive the reactor's state space equation, the reactor is first discretized in the axial direction as in Figure 3 in which inputs, output, and state variables for a segment are shown. Equations (3), (4), and (5) that pertain to spatial derivatives are discretized spatially, but governing equations (1) and (2) are still in the continuous form after discretization.

Equations (3), (4), and (5) which are governing equations for C_{NH_3} , C_{NO} , and T_g are discretized in the axial direction (x-direction in the equations). In this procedure, the state variables, and $T_{w,i}$ are assumed to be constant in each segment.

Using the first-order implicit Euler method, gas temperature output of i^{th} segment can be expressed as

$$\frac{T_{g,i+1} - T_{g,i}}{\Delta x} = T_{g,i} - \frac{h \cdot P}{\rho_g A_g C_{p,g} u} (T_{g,i+1} - T_{w,i}) \quad (6)$$

Where, subscription i , is an index for segmentation, and state variable $T_{w,i}$, is assumed to be a constant in the i^{th} segment. Therefore, gas temperature output of i^{th} segment is expressed as follows:

$$T_{g,i+1} = \left(\frac{\rho_g A_g C_{p,g} u}{\rho_g A_g C_{p,g} u + h \cdot P \cdot \Delta x} \right) \cdot T_{g,i} + \left(\frac{h \cdot P \cdot \Delta x}{\rho_g A_g C_{p,g} u + h \cdot P \cdot \Delta x} \right) \cdot T_{w,i} \quad (7)$$

Similarly, a discretized form of the species equations of gas-phase Ammonia and Nitrogen Monoxide (equations 3 and 4) are expressed as

$$C_{NH_3,i+1} = \frac{A_g u}{A_g u + s \Delta x \cdot p_a \cdot (1-\theta_i)} C_{NH_3,i}$$

$$+ \frac{s \cdot \Delta x \cdot p_d}{A_g u + s \Delta x \cdot p_a \cdot (1-\theta_i)} \exp\left(\frac{-E_{d0}(1-\alpha\theta_i)}{R \cdot T_w}\right) \cdot \theta_i \quad (8)$$

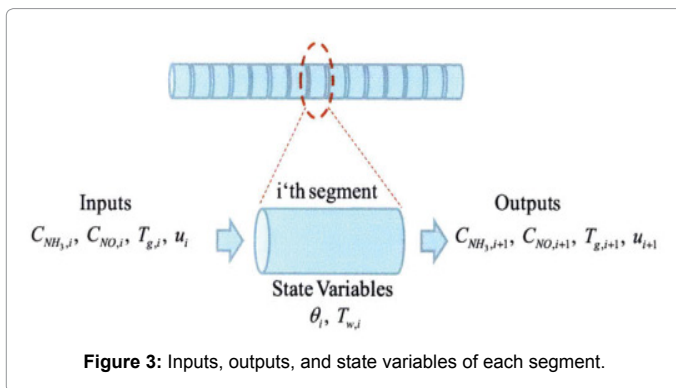


Figure 3: Inputs, outputs, and state variables of each segment.

$$C_{NO,i+1} = \frac{A_g u}{A_g u + s \cdot \Delta x \cdot p_r \cdot \exp\left(-\frac{E_r}{R \cdot T_{w,i}}\right)} C_{NO,i} \quad (9)$$

Equations 2 and 5 after discretization, are expressed as

$$\frac{\partial \theta_i}{\partial t} = (R_{a,i} - R_{d,i} - R_{r,i} - R_{o,i})$$

$$= \begin{pmatrix} p_a(1-\theta)C_{NH_3,i} - p_d \exp\left(-\frac{E_{d0}(1-\alpha\theta_i)}{R \cdot T_{w,i}}\right) \theta_i \\ -p_r \exp\left(-\frac{E_r}{R \cdot T_{w,i}}\right) \cdot \theta_i \cdot C_{NO,i} - p_o \exp\left(-\frac{E_o}{R \cdot T_{w,i}}\right) \cdot \theta_i \cdot C_{O_2} \end{pmatrix} \quad (10)$$

$$\frac{\partial T_{w,i}}{\partial t} = -\frac{h \cdot P}{\rho_w A_w C_{p,w}} (T_{w,i} - T_{g,i}) \quad (11)$$

Next step is to linearize the five governing equations, two of which are continuous in time domain and three of which are discretized in the space, around an equilibrium point that is determined using nominal input conditions. The equilibrium point for each segment i is determined by $C_{NH_3,i,eq}$, $C_{NO,i,eq}$, $\theta_{i,eq}$, $T_{w,i,eq}$, $T_{g,i,eq}$, and $u_{i,eq}$. These, in turn, are determined by supplying a constant $C_{NH_3,in}$, $C_{NO,in}$, $T_{g,in}$ and $u_{in,eq}$ with the resulting steady-state values of the i^{th} segment set as the corresponding equilibrium point. Using these equilibrium points, Equations (10) and (11) can be linearized around equilibrium points as follows:

$$\frac{\partial(\delta\theta_i)}{\partial t} = J_{11,i} \cdot \delta\theta_i + J_{12,i} \cdot \delta T_{w,i}$$

$$+ J_{13,i} \cdot \delta C_{NH_3,i} + J_{14,i} \cdot \delta C_{NO,i} \quad (12)$$

$$\frac{\partial(\delta T_{w,i})}{\partial t} = J_{22,i} \cdot \delta T_{w,i} + J_{25,i} \cdot \delta T_{g,i} \quad (13)$$

where $J_{kl,i}$ means that partial derivative of a k^{th} index variable with respect to l^{th} index variable under equilibrium in i^{th} segment. Variables indexed by k and l include the following: (Table 1).

- 1: θ
- 2: T_w
- 3: C_{NH_3}
- 4: C_{NO}
- 5: T_g
- 6: u

From Equations (12) and (13), system matrix for the i^{th} segment can be expressed as follows:

Before Discretization for the whole reactor	After Discretization for each segment
$\frac{\partial \theta}{\partial t} = (R_a - R_d - R_r - R_o)$	$\frac{\partial \theta_i}{\partial t} = (R_{a,i} - R_{d,i} - R_{r,i} - R_{o,i})$
$\frac{\partial T_w}{\partial x} = -\frac{h \cdot P}{\rho_w A_w C_{p,w}} (T_w - T_g)$	$\frac{\partial T_{w,i}}{\partial x} = -\frac{h \cdot P}{\rho_w A_w C_{p,w}} (T_{w,i} - T_{g,i})$
$\frac{\partial C_{NH_3}}{\partial x} = \frac{s}{A_g u}$ $\left(\begin{matrix} -P_a(1-\theta)C_{NH_3} \\ +P_d \exp\left(-\frac{E_{d0}(1-\alpha\theta)}{R \cdot T_w}\right)\theta \end{matrix} \right)$	$C_{NH_3,i+1} = \frac{A_g u}{A_g u + s \Delta x \cdot p_a \cdot (1-\theta_i)} C_{NH_3,i}$ $+ \frac{s \cdot \Delta x \cdot p_d}{A_g u + s \Delta x \cdot p_a \cdot (1-\theta_i)} \exp\left(\frac{-E_{d0}(1-\alpha\theta_i)}{R_u \cdot T_w}\right) \cdot \theta_i$
$\frac{\partial C_{NO}}{\partial x} = \frac{s}{A_g u}$ $\left(-P_r \exp\left(-\frac{E_r}{R \cdot T_w}\right) \cdot \theta \cdot C_{NO} \right)$	$C_{NO,i+1} = \frac{A_g u}{A_g u + s \cdot \Delta x \cdot p_r \cdot \exp\left(-\frac{E_r}{R_u \cdot T_{w,i}}\right)} C_{NO,i}$ $\cdot \theta_i$
$\frac{\partial T_g}{\partial x} = -\frac{h \cdot P}{\rho_g A_g C_{p,g} u} (T_g - T_w)$	$T_{g,i+1} = \left(\frac{\rho_g A_g C_{p,g} u}{\rho_g A_g C_{p,g} u + h \cdot P \cdot \Delta x} \right) \cdot T_{g,i}$ $+ \left(\frac{h \cdot P \cdot \Delta x}{\rho_g A_g C_{p,g} u + h \cdot P \cdot \Delta x} \right) \cdot T_{w,i}$

Table 1: Governing equations before and after discretization.

$$\frac{d}{dt} \begin{pmatrix} \delta \theta_i \\ \delta T_{w,i} \end{pmatrix} = \begin{bmatrix} J_{11,i} & J_{12,i} \\ 0 & J_{22,i} \end{bmatrix} \begin{pmatrix} \delta \theta_i \\ \delta T_{w,i} \end{pmatrix} + \begin{bmatrix} J_{13,i} & J_{14,i} & 0 & 0 \\ 0 & 0 & J_{25,i} & 0 \end{bmatrix} \begin{pmatrix} \delta C_{NH_3,i} \\ \delta C_{NO,i} \\ \delta T_{g,i} \\ \delta u_i \end{pmatrix} \quad (14)$$

This is in turn, $x_i = A_i x_i + B_i u$ (15)

Where,

$$x_i = \begin{pmatrix} \delta \theta_i \\ \delta T_{w,i} \end{pmatrix},$$

$$A_i = \begin{bmatrix} J_{11,i} & J_{12,i} \\ 0 & J_{22,i} \end{bmatrix},$$

$$B_i = \begin{bmatrix} J_{13,i} & J_{14,i} & 0 & 0 \\ 0 & 0 & J_{25,i} & 0 \end{bmatrix}, u_i = \begin{pmatrix} \delta C_{NH_3,i} \\ \delta C_{NO,i} \\ \delta T_{g,i} \\ \delta u_i \end{pmatrix}$$

In order to obtain the output equation for the i^{th} segment, governing

Equations (8), (9), and (7) should be linearized around equilibrium point as follows:

$$\delta C_{NH_3,i+1} = \frac{\partial C_{NH_3,i+1}}{\partial \theta_i} \delta \theta_i + \frac{\partial C_{NH_3,i+1}}{\partial T_{w,i}} \delta T_{w,i} + \frac{\partial C_{NH_3,i+1}}{\partial C_{NH_3,i}} \delta C_{NH_3,i} + \frac{\partial C_{NH_3,i+1}}{\partial u} \delta u$$

$$= J_{31,i} \delta \theta_i + J_{32,i} \delta T_{w,i} + J_{33,i} \delta C_{NH_3,i} + J_{36,i} \delta u \quad (16)$$

$$\delta C_{NO,i+1} = \frac{\partial C_{NO,i+1}}{\partial \theta_i} \delta \theta_i + \frac{\partial C_{NO,i+1}}{\partial T_{w,i}} \delta T_{w,i} + \frac{\partial C_{NO,i+1}}{\partial C_{NO,i}} \delta C_{NO,i} + \frac{\partial C_{NO,i+1}}{\partial u} \delta u$$

$$= J_{41,i} \delta \theta_i + J_{42,i} \delta T_{w,i} + J_{44,i} \delta C_{NO,i} + J_{46,i} \delta u \quad (17)$$

$$\delta T_{g,i+1} = \frac{\partial T_{g,i+1}}{\partial T_{w,i}} \delta T_{w,i} + \frac{\partial T_{g,i+1}}{\partial T_{g,i}} \delta T_{g,i} + \frac{\partial T_{g,i+1}}{\partial u_i} \delta u_i \quad (18)$$

The output equations can be summarized from equations (16), (17), and (18) as follows:

$$\begin{pmatrix} \delta C_{NH_3,i+1} \\ \delta C_{NO,i+1} \\ \delta T_{g,i+1} \\ \delta u_{i+1} \end{pmatrix} = \begin{bmatrix} J_{31,i} & J_{32,i} \\ J_{32,i} & J_{32,i} \\ 0 & J_{33,i} \\ 0 & 0 \end{bmatrix} \begin{pmatrix} \delta \theta_i \\ \delta T_{w,i} \end{pmatrix} + \begin{bmatrix} J_{33,i} & 0 & 0 & J_{36,i} \\ 0 & J_{34,i} & 0 & J_{46,i} \\ 0 & 0 & J_{35,i} & J_{55,i} \\ 0 & 0 & 0 & 1 \end{bmatrix} \begin{pmatrix} \delta C_{NH_3,i} \\ \delta C_{NO,i} \\ \delta T_{g,i} \\ \delta u_i \end{pmatrix} \quad (19)$$

This is, in turn, expressed compactly as:

$$y_i = C_i x_i + D_i u \quad (20)$$

$$y_i = \begin{pmatrix} \delta C_{NH_3,i+1} \\ \delta C_{NO,i+1} \\ \delta T_{g,i+1} \\ \delta u_{i+1} \end{pmatrix}, x_i = \begin{pmatrix} \delta \theta_i \\ \delta T_{w,i} \end{pmatrix}, u_i = \begin{pmatrix} \delta C_{NH_3,i} \\ \delta C_{NO,i} \\ \delta T_{g,i} \\ \delta u_i \end{pmatrix},$$

Where,

$$C_i = \begin{bmatrix} J_{31,i} & J_{32,i} \\ J_{32,i} & J_{32,i} \\ 0 & J_{33,i} \\ 0 & 0 \end{bmatrix}, D_i = \begin{bmatrix} J_{33,i} & 0 & 0 & J_{36,i} \\ 0 & J_{34,i} & 0 & J_{46,i} \\ 0 & 0 & J_{35,i} & J_{55,i} \\ 0 & 0 & 0 & 1 \end{bmatrix}$$

State Space Equation for the Entire System

After we first carried out a discretization and linearization procedure to convert the nonlinear PDEs into the linear system, we assembled state space equations for each segment into a single, large, state space equation. External inputs include $C_{NH_3}^{in}$, $C_{NO,in}$, $T_{g,in}$ and u_{in} , the inputs to the first segment, while system outputs are the outputs of the N^{th}

$$y_i = C_i x_i + D_i u_i$$

$$C_i = \begin{bmatrix} J_{31,i} & J_{32,i} \\ J_{41,i} & J_{42,i} \\ 0 & J_{52,i} \\ 0 & 0 \end{bmatrix}, D_i = \begin{bmatrix} J_{33,i} & 0 & 0 & J_{36,i} \\ 0 & J_{44,i} & 0 & J_{46,i} \\ 0 & 0 & J_{55,i} & J_{56,i} \\ 0 & 0 & 0 & 1 \end{bmatrix}$$

$i+1^{th}$ values which correspond to $C_{NH_3,i+1}$, $C_{NO,i+1}$ and $T_{g,i+1}$ are computed by the following equations:

The state variables $T_{w,i}$ and θ_i are assumed to be constant in each segment.

$$C_{NH_3,i+1} = \frac{A_g u}{A_g u + s \Delta x \cdot p_a \cdot (1 - \theta_i)} C_{NH_3,i} + \frac{s \cdot \Delta x \cdot p_d}{A_g u + s \Delta x \cdot p_a \cdot (1 - \theta_i)} \exp\left(\frac{-E_{d0}(1 - \alpha \theta_i)}{R_u \cdot T_w}\right) \cdot \theta_i$$

$$C_{NO,i+1} = \frac{A_g u}{A_g u + s \cdot \Delta x \cdot p_r \cdot \exp\left(-\frac{E_r}{R_u \cdot T_{w,i}}\right)} C_{NO,i}$$

$$T_{g,i+1} = \left(\frac{\rho_g A_g C_{p,g} u}{\rho_g A_g C_{p,g} u + h \cdot P \cdot \Delta x}\right) \cdot T_{g,i} + \left(\frac{h \cdot P \cdot \Delta x}{\rho_g A_g C_{p,g} u + h \cdot P \cdot \Delta x}\right) \cdot T_{w,i}$$

Substituting the parameters in the above equations will give

$$C_{NH_3,i+1} = 0.907 C_{NH_3,i} + 6.9615 \times 10^{-15}$$

$$C_{NO,i+1} = 0.9999 C_{NO,i}$$

$$T_{g,i+1} = 0.632 T_{g,i} + 183.2$$

The concentration of Ammonia and Nitrogen oxide in ppm is 330.

Analyzing the dynamics of a segment

The system matrix A_1 is computed from the Jacobians associated with it (Tables 2 and 3).

$J_{11,i}$	$-0.25 C_{NH_3,i} - 6.46 \times 10^{-4}$
$J_{12,i}$	$-0.0208 C_{NO,i} - 6.153 \times 10^{-8}$
$J_{22,i}$	-0.4583
$J_{13,i}$	0.2498
$J_{14,i}$	-4.264×10^{-4}
$J_{25,i}$	0.4583
$J_{31,i}$	$0.0845 C_{NH_3,i} + 3.986 \times 10^{-4}$
$J_{32,i}$	4.31×10^{-11}
$J_{41,i}$	$-1.17 \times 10^{-13} C_{NO,i}$
$J_{42,i}$	$-2.73 \times 10^{-18} C_{NO,i}$
$J_{33,i}$	0.907
$J_{52,i}$	0.36787
$J_{44,i}$	0.9998
$J_{55,i}$	0.632
$J_{36,i}$	$2.516 C_{NH_3,i} - 1.85 \times 10^{-8}$
$J_{46,i}$	$0.0024 C_{NO,i}$
$J_{56,i}$	0.632
$J_{66,i}$	1

Table 2: Jacobians associated with the state space equations with practical parameters.

$$A_1 = \begin{bmatrix} -8.475 \times 10^{-4} & -1.693 \times 10^{-5} \\ 0 & -0.4583 \end{bmatrix}$$

The Eigen values of A_1 are observed to be -0.00084 and -0.4583 .

Both the poles of the system matrix corresponding to A_1 are on the right side of the s-plane and the system is stable.

Analyzing the system -30th order linear model

The non-linear model is linearized to obtain the 30th order model computed from the equations 19, 20 with, $C_{NO,i}$ and $T_{g,i}$ values regularly updated for each segment starting from input to the output.

The MATLAB code to compute the 30th order system matrix is listed in the Appendix section. The Eigen values for the system are found to be -Eigen values of $A_{30 \times 30}$ system matrix- $[-0.000697 -0.000702 -0.000709 -0.000715 -0.000722 -0.000730 -0.000734 -0.000745 -0.000756 -0.000770 -0.000783 -0.000797 -0.000812 -0.000829 -0.000848 -0.4583 -0.4583 -0.4583 -0.4583 -0.4583 -0.4583 -0.4583 -0.4583 -0.4583 -0.4583 -0.4583 -0.4583 -0.4583 -0.4583 -0.4583 -0.4583]$.

It can be observed that the all the 30 poles are real and negative. The poles are placed in the negative half of the s-plane. The system is stable (Figure 5).

From the Eigen values plot, we can observe that the poles of the system are repetitive and many of them are almost closely placed. This also means that the system order can be reduced preserving the dynamics of the original system.

Reduced order system dynamics

Reducing the main interface to model approximation algorithms.

$C_{NH_3,in}$	8.11×10^{-4}
$C_{NO,in}$	8.11×10^{-4}
$C_{O_2,in}$	1.96616

Table 3: Concentrations NH_3 , NO , and O_2 at the input.

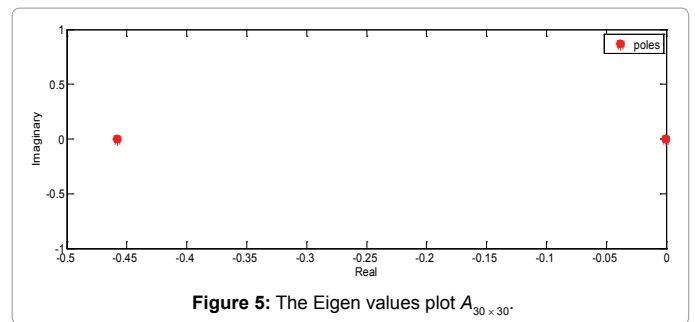


Figure 5: The Eigen values plot $A_{30 \times 30}$.

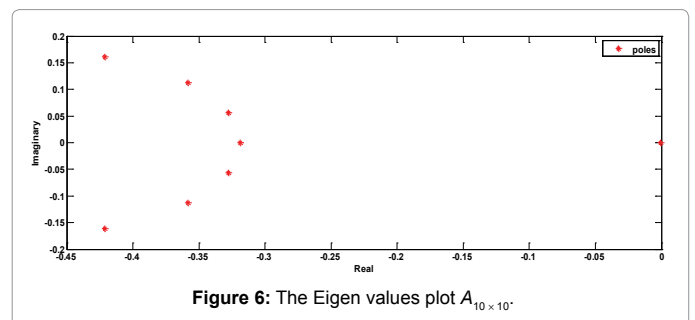


Figure 6: The Eigen values plot $A_{10 \times 10}$.

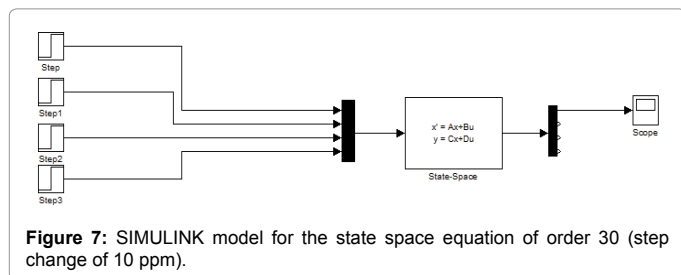


Figure 7: SIMULINK model for the state space equation of order 30 (step change of 10 ppm).

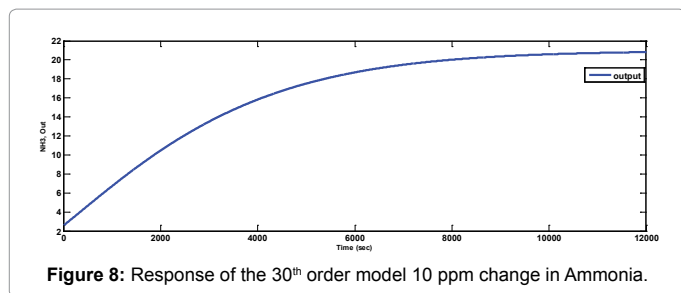


Figure 8: Response of the 30th order model 10 ppm change in Ammonia.

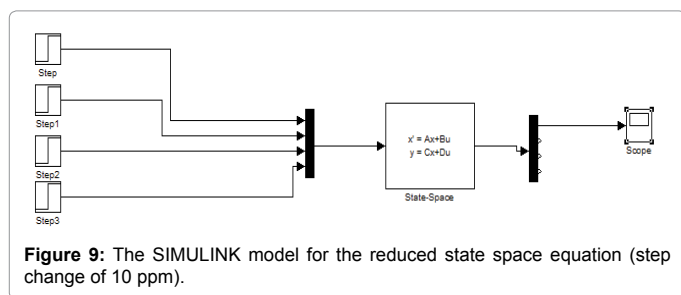


Figure 9: The SIMULINK model for the reduced state space equation (step change of 10 ppm).

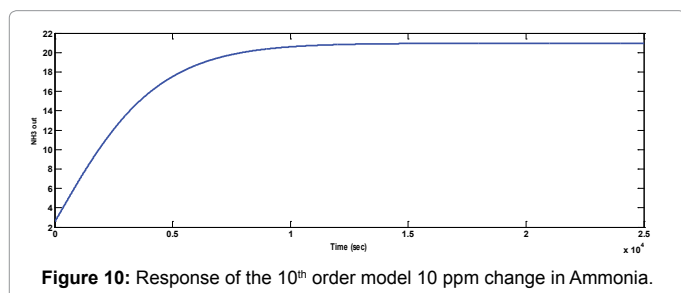


Figure 10: Response of the 10th order model 10 ppm change in Ammonia.

Reducing the 30th order linear model into 10th order using Hankel SV model reduction [27]. Hankel singular values of a stable system indicate the respective state energy of the system. Hence, the reduced order can be directly determined by examining the system Hankel SV's. Model reduction routines, which based on Hankel singular values are grouped by their error bound types. In many cases, the additive error method GRED=reduce (G, ORDER) [in MATLAB] is adequate to provide a good reduced order model which reduces the relative errors between G and GRED tends to produce a better fit.

In this paper, the order of the system is reduced to 10 to analyze its dynamics in that order.

Eigen values: [-0.4211+0.1614i, -0.4211-0.1614i, -0.3583+0.1126i, -0.3583-0.1126i, -0.3278+0.0569i, -0.3278-0.0569i, -0.3186, -0.00052, -0.00058+0.000154i, -0.00058-0.000154i] (Figures 6-10).

Results

Output comparison of the 30th order and the reduced 10th order models: The outputs of both the 30th order and 15th order systems are analyzed for a step change of 10 ppm in the concentration of Ammonia while all the other parameters remain same.

From both the above plots (in Figures 7 and 9) it is reasonably inferred that the response of the reduced order model is similar to the original 30th order model. The steady state output values of NH₃ in both responses are nearly the same. For a sufficiently higher model, the dynamics of the reduced order model is expected to be the same as the higher order model with minimum errors.

Conclusion

Nonlinear models are derived based on physical and chemical interpretation of the catalyst and certain simplifications. We subsequently discretized and linearized the nonlinear equations and analyzed the system dynamics of the catalyst. The following are some of our main observations regarding the SCR dynamic model:

- The steady state output of the first principle-based model given sufficiently accurate results for a higher order linear system. Order of 30 is chosen for satisfactory accuracy in results
- The dynamics of the reduced order system is the same as the higher order linear model. Since many poles are repetitive, the system can be reduced to a degree which gives an almost the same response as the higher order model also keeping in view of the errors involved in the reduction method. Dynamics of settling time and trend are seen to be the same for both the models
- Although the model of the SCR developed during this thesis was for an extruded Vanadia formulation, the SCR model can be easily applied to other catalyst formulations e.g. Copper-Zeolite. This would, however, require that tests be conducted on the chosen formulations to identify the significant chemical kinetics. The model offers flexibility to model additional reactions or remove unnecessary reaction kinetics.

Acknowledgement

I wholeheartedly thank Dr. M Umapathy, Professor, Instrumentation and Control Engineering, NIT Trichy., for his constant support and guidance, and without whom the completion of this project in fruition would not have been possible.

References

1. JN Chi, HFM DaCosta (2005) Modeling and control of a Urea-SCR after treatment system. SAE Tech Paper 1: 0966.
2. L Lietti, I Nova, S Camurri, E Tronconi, P Forzatti (1997) Dynamics of the SCR-DeNO_x reaction by the transient-response method. AIChE J 43:2559-2570.
3. JY Kim, G Cavataio, JE Patterson, PM Laing, CK Lambert (2007) Laboratory studies and mathematical modeling of urea SCR catalyst performance. SAE Tech Paper 1: 1573.
4. Hanbee Na (2010) Physics based modeling of urea selective catalytic Reduction Systems.
5. Ramachandra R, Ramesh S (2014) Ammonia dosing control strategy for heavy duty automotive SCR. Automotive Engineering Chalmers University of Technology.
6. <https://in.mathworks.com/help/robust/ref/reduce.html>